Heat transfer characteristics in forced convection through a rectangular channel with broken V-shaped rib roughened surface

2015 J. Phys.: Conf. Ser. 655 012060

(http://iopscience.iop.org/1742-6596/655/1/012060)

Journal of Physics: Conference Series **655** (2015) 012060 doi:10.1088/1742-6596/655/1/012060

Heat transfer characteristics in forced convection through a rectangular channel with broken V-shaped rib roughened surface

D Fustinoni, P Gramazio, L Colombo and A Niro
Politecnico di Milano, Department of Energy,
Campus Bovisa, Via Lambruschini 4, 20156 Milano, Italy

Corresponding author email: alfonso.niro@polimi.it

Abstract. In this paper we present experimental results for a rectangular channel with the lower and upper walls configured with V-shaped broken ribs pointing both upward and downward the flow stream, as well as in a mixed configuration. Results for V-shaped ribs upward pointing are also reported for comparison. The duct cross-section is 120-mm wide and 12-mm height; the rib-roughened walls are operated at fixed temperature whereas the channel side walls are adiabatic. The ribs have square cross section of 2 mm in side, a V-apex angle of 60°, and a pitch-to-side ratios of 10 and 40. Reynolds number has been varied between 700 and 7500. The results show that the flow regime seems to be turbulent even at the lowest tested value of Re, and the friction factor is quite independent of Re, i.e., the typical trend for k-roughened surfaces. Broken and continued ribs seems to perform with no evident differences between them, except at the lowest values of Re while prevailing the former or the latter according to *p/e*. Anyway, adopting ribbed surface is always advantageous and allows a maximum heat transfer enhancement factor of 4.9.

1. Introduction

In many leading-edge engineering components the best performances entail high heat transfer rates, frequently in order to avoid the temperature overcoming limits in some their critical points, such as in gas-turbine blade cooling. Thus, very efficient and stable cooling systems are required to ensure a good operation and durability of these devices. To this end, many passive techniques to enhance heat transfer have been studied [1], [2] and, among them, the rib-roughened surfaces because they are reliable, robust, effective and quite inexpensive. As the possible shapes and arrangements of ribs are countless, starting from the ‘70s, a continuously growing number of studies have been dealing with heat transfer over this kind of enhanced surfaces.

From the ‘90s several studies, such as Han et al. [3], Kukreja et al. [4] and Gao and Sunden [5], have been devoted to V-shaped ribs as they are supposed to be effective in enhancing secondary flows. Han et al. in [3] found that the V-shaped ribs with apex angle of 45° and 60° are more effective than the parallel-tilted ribs with the same angles; besides, they also found the arrangements with the V-apex pointing upward the main flow stream are more effective than the contrary ones. However, Gao and Sunden in [5] asserted just the opposite.

From the same ‘90s, some studies also started proposing V-shaped broken rib configurations, namely, V-shaped ribs with the last part of their branches detached and staggered, because this kind of ribs was

expected to promote more cells of secondary flows than the V-shaped "continued ribs", and that in turn should increase local turbulence and, subsequently, heat transfer.
Actually, Han and Zhang [6] found that the V-shaped broken ribs, inside a channel with a square cross-section and uniformly heated walls, promoted a higher heat transfer augmentation than the V-shaped "continued ribs". Liou et al. in [7] reported the results of a study on twelve different configurations, with both continuous and broken transverse-, tilted-, V-shaped-ribs mounted only on one wall of a channel with a square cross-section; however, they found the highest heat transfer increase is generated by the use of continuous V-shaped ribs.
Again, also in this case, we can't draw a definitive conclusion whether V-shaped broken ribs perform better or not than continued one, because the performances depend on many factors. For this reason, we started an experimental campaign aimed at investigating heat transfer characteristics and pressure drops inside a rectangular channel, with the lower and upper walls configured with a large variety of ribs.

2. Experimental setup

As schematically shown in figure 1(a), the experimental setup consists of two independent circuits, namely, the air-circuit containing the test section, and the heating-water circuit used to control the temperature of the channel walls.

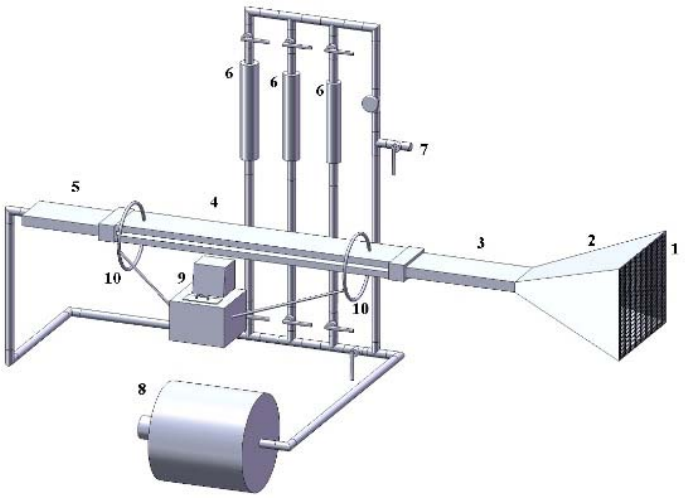

Figure 1(a). Schematics of the experimental setup: 1. fine mesh screen cover; 2. convergent air inlet; 3. entry-section; 4. test-section; 5. exit-section; 6. rotameters; 7. by-pass; 8. blower; 9. thermostatic bath; 10. water circuit piping.

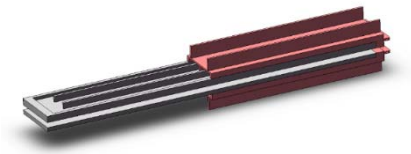

Figure 1(b). Test section with the duct on the wall backside.

Through a convergent duct, room air flows into the circuit; a fine mesh screen covers the convergent entrance, whereas at its exit there is a flow straightener consisting in a matrix of staggered 4-mm-diameter, 40-mm long thin polystyrene tubes. Inside the convergent a PTR is mounted to measure the air temperature. From the straightener air flows into an entry-section that is a rectangular duct with the same cross-section dimensions as the tested channel; entry-section is 0.8-m long, i.e., near 40 times the channel hydraulic diameter, and its walls are made with 10-mm thick plexiglass plates and are not heated. At the end of this section, air enters the test-section that is a 120-mm wide, 12-mm height, 880-mm long duct; its lower and upper walls are two aluminium plates of 10-mm minimum thickness with a rib configured face.
As shown in figure 1(b), the backside of each plate is covered by a cap strongly tightened to the plate, so that they form a jacket where the heating water flows. Inside and outside the water jacket there are

ribs which prevent the plate buckling. To check if temperature is uniform over the heated walls, four thermocouples are embedded in the lower wall and three in the upper one; each thermocouple is cemented into a 1.8-mm-wide, 0.5-mm-depth groove cut in the flat face. Eventually, the test-section sides are closed by 4-mm-thick glass plates to allow optical access inside the channel.
At the test-section exit, there is a short exit-section equipped with two turbolizer rows followed by a convergent that conveys air through a 20-mm-wide, 6-mm-high channel partially filled by a fine-meshed plastic net; after the screen, a PTR and a thermocouple are positioned on the centreline of this channel to measure the air bulk-temperature. Finally, inside the couplings between the entry-section and the test-section, and between this one and the exit-section there are two pressure taps, each consisting in a 1.5-mm-diameter hole (great care was devoted in eliminating any burr). Downstream the exit-section there are three rotameters, i.e., float-type flow-meters, connected in parallel with full scale of 6, 23.5 and 40 m³/h respectively, a metering valve, and a 7-stage, 30-kPa-head, 5.5-kW-power blower operating in suction mode. The exhausted air is discharged outside the laboratory. Air temperature is also measured upstream the flow-meters by means of a thermocouple plugged in the pipe.
The heating circuit is mainly composed by a heat bath which provides high mass flow-rate of water at constant temperature, and by the channels built into the upper and lower test-section walls (water and air stream in counterflow); two thermocouples are placed inside each water channel, near the inlet and outlet ports, respectively. The heat bath is the ThermoHaake B12 with a tank of 12-dm³, a 3-kW heater and a high precision controller; water temperature inside the tank is kept constant within 0.01 K.

3. Measurements, data processing and error analysis

All the thermocouples here used are T-type with 0.5-mm-diameter wires, whereas the PTR are 4-wires, 100-ohm, Platinum type, i.e., PT100, with dimensions of 2 mm x 4 mm. Both thermocouples and PTR were all preliminary calibrated over five points within the temperature range from 22 to 60 °C, by means of the ThermoHaake heat bath. The probes were immersed all together into the bath while devoting great care in their positioning; for each calibration point, 160 readings per probe were collected; the resulting standard deviation is of 0.02 K for the thermocouples, and of 0.01 K for the thermo-resistances. All temperature measurements are performed by means of an Agilent 34970A data logger equipped with a relay multiplexer and a 6½ digit multimeter. The channels are sequentially read, by waiting a 0.5-s settling time after each channel-locking, with an integration time of 400 ms which ensures a standard deviation of 0.01 K that is less than or equal to the probe uncertainties; consequently, reading cycles are performed every 20 s. Pressure drops are measured by connecting the two pressure taps, placed at the inlet and outlet of the test channel, to a differential micromanometer with a full scale of 250 Pa and a 0.125-Pa sensitivity. Air volume-flow-rate is measured by means of the aforementioned rotameters which have a 2% nominal accuracy; however, by means of a calibration performed by measuring pressure drops of laminar air-flows through a smooth circular tube, we found that their accuracy is better of 1%. Finally, in order to guarantee repeatability to measurements, we adopted a precise test procedures described in the following. First, we power the bath heater and water starts to circulate through the entire circuit included the ducts on the test-section wall backside. After 30 minutes, that is the time to stabilize the channel wall temperature to a prefixed value within a 0.01-K band, we power the blower and air starts to flow through the test section. Then we need to wait for other 30 minutes in order to attain regime conditions with all temperature time-fluctuations within 0.02-K band; in this conditions, channel wall-temperature is uniform within 0.1 K over the entire heated length. Eventually, we start to collect 20 reading-cycles which take 400 s; during this time, measurements of the air-volume-flow-rate and of reading-cycles was chosen first by collecting data for N=200 for some of the most representative regime conditions, and then by calculating their average standard deviation as a function of N; as a result, we found that at N=20 the average standard deviation becomes less than 0.01 K, and thus we assumed that 20 is the minimum reading-cycle number to be collected.
The average Nusselt over the test section and the Darcy-Weisbach friction factor are calculated as follows

$$Nu = \frac{hD_H}{k},\ \mathrm{Re} = \frac{\rho u D_H}{\mu} \tag{1}$$

$$h = \frac{\dot{Q}/A_S}{\Delta T_{m,Log}} = \frac{\dot{m}c_p(\theta_i - \theta_o)}{A_S[(\theta_i - \theta_o)/\ln(\theta_i - \theta_o)]} = \frac{\rho \dot{V} c_P}{A_S} \ln\frac{\theta_i}{\theta_o} \tag{2}$$

$$Nu = \frac{D_H}{k}\frac{\rho \dot{V} c_P}{A_S}\ln\frac{\theta_i}{\theta_o},\ \mathrm{Re} = \frac{\rho \dot{V} D_H}{A\mu} \tag{3}$$

$$f = \frac{\Delta p}{\rho u^2/2}\frac{D_H}{\ell_{taps}} = \frac{2\Delta p A^2 D_H}{\rho \dot{V}^2 \ell_{taps}} \tag{4}$$

where h the average convective coefficient, $\dot{Q}$ the total heat power exchanged, A and A_S the cross-section area and the total heated area, respectively, of the test section, $D_H=2A/(w+H)$ the channel hydraulic diameter, the log-mean-temperature difference, θ_i and θ_o the wall-to-air-bulk-temperature difference at the entrance and exit, respectively, of the test section, and $\dot{V}$ the mass-flow-rate and the volume-flow-rate of air, respectively, ρ the density calculated at the temperature where is measured, c_p the specific heat at constant pressure and k the thermal conductivity of air, Δp the pressure drop, and ℓ_{taps} the distance between the pressure taps.

The error analysis performed according to Moffat [8] gives an uncertainty less than 3% on the convective coefficient, and less than 7% on the apparent Darcy friction factor.

4. Results

All data here reported refer to a rectangular channel with aspect ratio of 0.1, and to air-flows entering at room temperature, namely, about 22 °C. Heat transfer characteristics refer to the test section operated with the lower and upper wall at uniform and fixed temperature at the nominal value of 40 °C, while friction factors are obtained with channel walls at room temperature. Table 1 shows the main dimension of the channel geometry.

Table 1. Main channel parameters.

Channel height, H	[mm]	12.00
Channel length, L	[mm]	880.00
Channel width, w	[mm]	120.00
Hydraulic diameter, D_H	[mm]	21.82
Height to width ratio	[-]	0.10

Tests have been carried out on broken V-shaped ribs pointing both upward and downward the main stream, referred to as 3D_Up and 3D_down respectively, and furthermore in a mixed configuration, with ribs on the lower wall pointing downward while upward the ones on the upper wall referred to as 3D_mix. In addition, results for V-shape continuous ribs pointing upward (V_up) are also here presented in order to evaluate differences between these two configurations. Figure 2 shows a schematic of the different tested configurations. All ribs have a square cross section, with a side dimension of 2 mm and a pith-to-side ratio equal to 10 and 40.

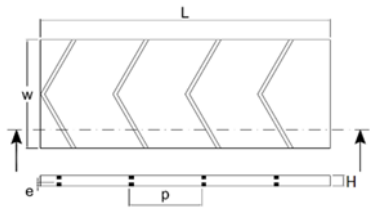

Figure 2(a). V_up: V-shaped ribs in upstream configuration.

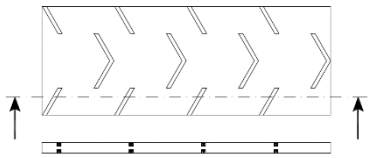

Figure 2(b). 3D_up and 3D_down: broken V-shaped ribs in upstream or downstream configuration.

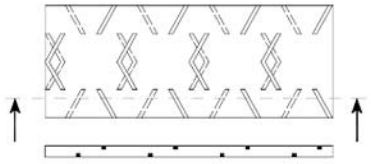

Figure 2(c). 3D_mix: broken V-shaped ribs in mixed upstream-downstream configuration.

In figures 3(a) and 3(b) the average Nusselt numbers over the test section, evaluated according to equation (3), are plotted versus Reynolds number for all ribs arrangements. As reference values, data for a flat channel with the same dimensions and operating conditions are also reported. Finally, as solid lines, the values predicted for a flat rectangular-channel by the Shah-London correlation, with the Wibulsas correction, for Re<2300, and by the Gnielinski correlation for Re≥2300 [9] are plotted in the same graph. All ribs configurations show an increasing trend from the lower investigated Reynolds number to the upper ones, and a power-law dependence on Re with an exponent of about 0.9. The absence of a region where Nusselt numbers are independent by Reynolds numbers indicates that flow regime is turbulent since the lower investigated Reynolds number. The highest heat transfer increase is for the broken V-shaped with downward apex and p/e=10, as it displays a mean value of the ratio Nu/Nu_0 equal to 3.0 (Nu_0 refers to the flat channel operated at the same conditions) with a maximum of 4.9 at Re=3250. Among the broken ribs, the arrangements with the downward apex always show values higher than the upward one, or the mixed configuration. With regard to the pitch-to-side ratio, the arrangements with p/e=10 perform better than p/e=40. It is noteworthy that broken V-shape with upward apex displays values of Nu higher than the mixed (broken) configuration for p/e=10 but lower than the latter for p/e=40. By comparing thermal performances of broken and continued ribs with upward apex, seemingly there are no differences between them except at the lowest Reynolds number where a opposite behaviour is displayed according to p/e. In particular, for p/e=10 continued ribs perform better than broken ones, but for p/e=40 the latter configuration is winning.

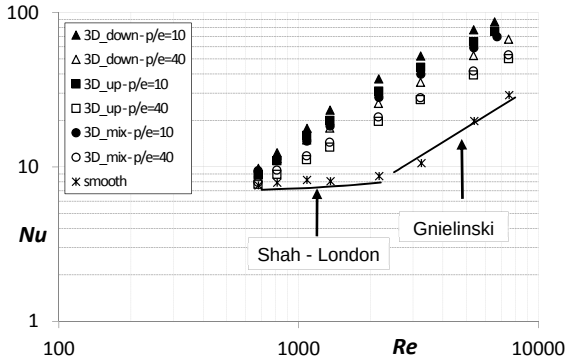

Figure 3(a). Average Nusselt number versus Reynolds number for the broken V-shaped arrangements.

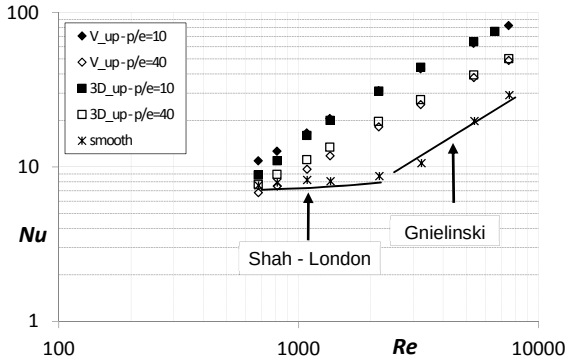

Figure 3(b). Average Nusselt number versus Reynolds number for the broken and continuous V-shaped pointing upward arrangements.

Figures 4(a) and 4(b) show experimental values of the apparent Darcy friction factor f plotted versus Re for all the rib configurations. For comparison, the figures also report as solid lines the values f_0 predicted for a flow through the flat rectangular channel, both in laminar regime and turbulent regime, by the Shah-London correlation [9]. All configurations show higher values of f than the smooth channel. In

particular, the highest value of ratio f/f_0 is 16 for broken V-shaped ribs, pointing both upward and downward, for p/e=10. Figures 4(a) shows that V-shaped ribs with both upward and downward apex display pressure drops higher than the mixed configuration. That always holds for p/e=10 whereas for p/e=40 it is true only at high Reynolds numbers. Comparison of data for broken and continued ribs shows the former has always values higher than the latter for p/e=10, while for p/e=40 there is a dependence on the Reynolds number, namely, f of broken ribs is higher than continued ones for Re<2100 while becoming lower in the fully-turbulent regime.

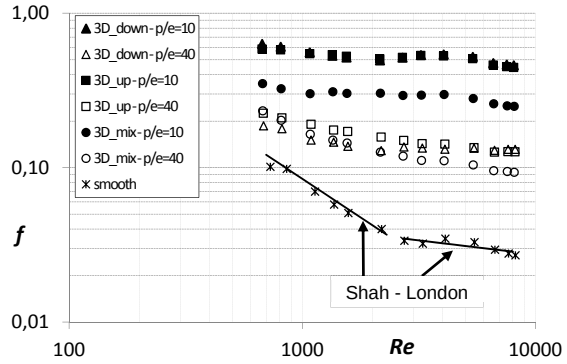

Figure 4(a). Darcy friction factor versus Reynolds number for the broken V-shaped arrangements.

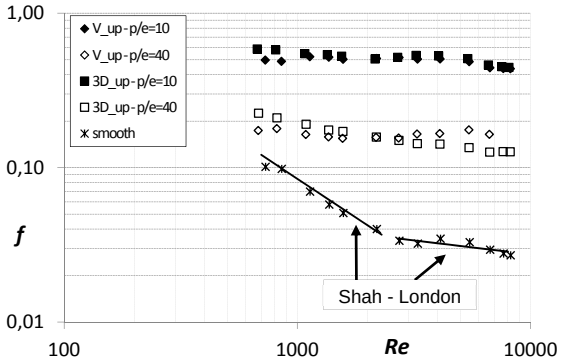

Figure 4(b). Darcy friction factor versus Reynolds number for the broken and continuous V-shaped pointing upward arrangements.

As a concluding remark, from an engineering point of view it is more interesting to compare performances of different rib configurations by taking into account simultaneously both heat transfer enhancement and pressure-drop penalization at constant pumping power, equation (5).

$$\frac{Nu/Nu_0}{(f/f_0)^{1/3}} \tag{5}$$

Figure 5 shows data obtained according to this criterion plotted versus the Reynolds number; all rib arrangements have similar trends with a maximum at Reynolds number of 3250. Broken V-shaped with apex pointing downward for p/e=40 seems to be the best configuration with the highest value of 2.07.

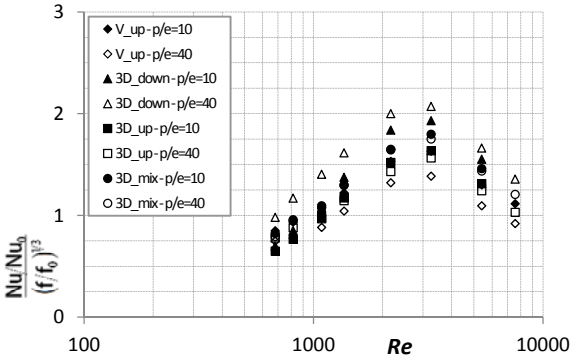

Figure 5. Heat exchangers comparison at constant pumping power.

On the other side the worst one is the continuous V-shaped pointing upward for p/e=40. According to this criterion, broken ribs perform better than continued ones over all the investigated Reynolds number

but only for *p/e*=40; it can be seen that the maximum values are 1.57 and 1.39, respectively. At the lowest pitch-to-side ratio, the difference seems to decrease.

5. Conclusions

Within the investigated range of Reynolds numbers, i.e., 700 – 7500, the configuration with broken V-shaped pointing downward for *p/e*=40 shows the best compromise between heat transfer enhancement and pressure drop penalization at constant pumping power. From the collected data, the following general conclusions can be drawn.

Average Nusselt number:

- data for all ribbed tested configurations show the flow regime seems to be turbulent even at the lowest tested value of *Re*, and a power law dependence on *Re* with an exponent of 0.9;
- the highest heat transfer enhancement factor is 4.9 at *Re*=3250 for V-shaped broken ribs pointing downward with *p/e*=10;
- V-shaped pointing downward arrangements seem to have larger values than other investigated configurations;
- data for broken and continued ribs seem to have no evident difference between them except at the lowest values of *Re*.

Pressure drop:

- data confirm the flow regime seems to be turbulent even at the lowest tested value of *Re*
- the highest value of the ratio f/f_0 is 16 and is attained by the V-shaped broken ribs, pointing both upward and downward, with *p/e*=10;
- mixed configuration is characterized by values lower than the others except for *p/e*=40 at the lowest *Re*.

6. Nomenclature

Symbol	Quantity	Unit
A	Channel cross section area	m^2
A_S	Channel total heated area	m^2
AR	Channel aspect ratio	-
c_p	Air specific heat at constant pressure	$J\ kg^{-1}\ K^{-1}$
D_H	Channel hydraulic diameter	m
e	Rib side dimension	mm
f	Darcy-Weisbach friction factor	-
H	Channel height	mm
h	Average convective coefficient	$W\ K^{-1}\ m^{-2}$
k	Air thermal conductivity	$W\ K^{-1}\ m^{-1}$
ℓ_{taps}	Distance between the pressure taps	m
$\dot{m}$	Air mass flow-rate	$kg\ s^{-1}$
Nu	Average Nusselt number	-
p	Rib pitch	mm
Δp	Pressure drop over ℓ_{taps}	Pa
Pr	Prandtl number	-
$\dot{Q}$	Total heat power exchanged	W
Re	Reynolds number	-
$\Delta T_{m,Log}$	Log-mean-temperature difference	K
$\dot{V}$	Air volume flow-rate	$m^3\ s^{-1}$
w	Channel width	mm
Greek symbols		
α	Rib angle respect to main stream	deg

θ	Wall-to-air-bulk-temperature difference	°C
ρ	Air density	kg m^{-3}
μ	Dynamic viscosity	kg m^{-1} s^{-1}

Subscripts

i	Inlet
o	Outlet
0	Performance of smooth channel

7. References

[1] Webb R L 1994 *Principles of enhanced heat transfer* (New York: Wiley-Interscience)
[2] Gupta S, Chaube A and Verma P 2012 Review on Heat Transfer Augmentation Techniques: Application in Gas Turbine Blade Internal Cooling *J. Eng. Sci. Tech. Rev.* **1** 57-62
[3] Han J C and Park J S 1985 Heat transfer enhancement in channels with turbulence promoters *J. Eng. Gas Turbines Power* **107** 628-35
[4] Kukreja R T, Lau S C and McMillin R D 1993 Local heat/mass transfer distribution in a square channel with full and V-shaped ribs *Int. J. Heat Mass Tran.* **36** 2013-20
[5] Gao X and Sunden B 2001 Heat transfer and pressure drop measurements in rib-roughened rectangular ducts *Exp. Therm. Fluid Sci.* **24** 25-34
[6] Han J C and Zhang Y M 1992 High performance heat transfer ducts with parallel broken and V-shaped broken ribs *Int. J. Heat Mass Tran.* **35** 513-23
[7] Liou T M, Chen C C and Tsai T W 1999 Heat transfer and fluid flow in a square duct with 12 different shaped vortex generators *J. Heat Transf.* **122** 327-35
[8] Moffat R J 1988 Describing the uncertainties in experimental results *Exp. Therm. Fluid Sci.* **1** 3-17
[9] Kakaç S, Shah R K and Aung W 1987 *Handbook of single-phase convective heat transfer* (New York: Wiley-Interscience)